Catalytic hydrogen evolution properties of nickel-doped tungsten disulfide

Andrzej Sobczynski, A. J. Bard, A. Campion, M. A. Fox, T. E. Mallouk, S. E. Webber, and J. M. White

J. Phys. Chem., **1989**, 93 (1), 401-403 • DOI: 10.1021/j100338a077

ruthenium complex and viologen to the micellar surface, the result being approximately equivalent radical yields whether in the presence or absence of SDS micelles. However, for $RuMC_5^{2+}/C_6V^{2+}$ and $RuMC_5^{2+}/C_{12}V^{2+}$ the breakup of the self-association of C_nV^{2+} by the SDS micelles dominates, and the radical yields decrease in the presence of SDS micelles.

The interaction between $RuMC_5^{2+}$ and C_nV^{2+} is not suggested to be intimate enough to allow rapid back-electron-transfer, since significant radical yields are observed. While the structural picture is rather imperfect, it does seem clear that alkyl chains on the electron donor and acceptor generate subtle ultrastructural changes that potentially allow control of the photoinduced electron-transfer efficiency.

Conclusions

The results in Figure 1 indicate a net electron transfer between photoexcited tris(bipyridine)ruthenium and methylviologen when bound to SDS micelles at 77 K. Based upon the similarity in ESR spectral properties, the observed signal is attributed to the viologen monocation radical. Noticeably absent from the ESR spectra was any indication of another radical species, which one would expect to arise from the oxidized ruthenium chromophore. Two very distinctive ESR spectra have been previously assigned to the $Ru(bpy)_3^{3+}$ radical,[17,18] either of which should have been easily recognized in the samples in the present study. Presumably, this other radical species is not stable in frozen micellar or frozen aqueous solutions.

The trends shown for the radical yields observed in the different samples indicate variability in the average separation distance between ruthenium and viologen molecules. One explanation of these trends is that both the ruthenium complex and the viologen molecule become embedded in the SDS micellar interface to varying degrees, depending on their alkyl chain length. This interpretation explains two major features of Figure 4. First, for the $Ru(bpy)_3^{2+}$ samples, the radical yield declines from MV^{2+} to $C_{20}V^{2+}$, suggesting that the viologen moiety is gradually being inserted more deeply into the micellar interface with increasing alkyl chain length, and thus is further away from the ruthenium chromophore.

Second, an optimal yield is found for the alkylruthenium complexes with C_6V^{2+} and C_8V^{2+}. One expects these complexes to be embedded deeper into the micelle, and optimum proximity to the alkylmethylviologens apparently occurs for hexyl to octyl.

In aqueous solutions without SDS micelles the differences in yields shown in Figure 5 are consistent with a scheme where the alkylmethyl viologens self-associate to form aggregates in frozen solution with larger aggregates for longer alkyl chains. The larger aggregates have a greater tendency to associate with $RuMC_5^{2+}$, but with $Ru(bpy)_3^{2+}$, association of the larger aggregates is modified by charge effects. In the presence of SDS micelles the C_nV^{2+} aggregates are broken up and the radical yields are affected accordingly.

Acknowledgment. This research was supported by the Division of Chemical Sciences, Office of Basic Energy Science, Office of Energy Research, U.S. Department of Energy. We thank Drs. D. H. P. Thompson and J. K. Hurst of the Oregon Graduate Center for generously providing the alkylmethylviologens.

Registry No. SDS, 151-21-3; $MVCl_2$, 1910-42-5; $Ru(bpy)_3Cl_2$, 14323-06-9; C_6VCl_2, 116911-79-6; C_8VCl_2, 116911-80-9; $C_{10}VCl_2$, 116911-81-0; $C_{12}VCl_2$, 74733-79-2; $C_{14}VCl_2$, 73605-96-6; $C_{16}VCl_2$, 75805-30-0; $C_{18}VCl_2$, 75805-29-7; $C_{20}VCl_2$, 116911-82-1; $RuMC_5$, 116926-82-0; $RuMC_{13}$, 116926-83-1; $RuMC_{17}$, 116926-84-2.

(17) DeSimone, R. E.; Drago, R. S. *J. Am. Chem. Soc.* **1970**, *92*, 2343. Quayle, W. H.; Lundsford, J. H. *Inorg. Chem.* **1982**, *21*, 97.
(18) Kennelly, T.; Gafney, H. D.; Braun, M. *J. Am. Chem. Soc.* **1985**, *107*, 4431.

Catalytic Hydrogen Evolution Properties of Nickel-Doped Tungsten Disulfide

Andrzej Sobczynski,† A. J. Bard, A. Campion, M. A. Fox, T. E. Mallouk, S. E. Webber, and J. M. White*

Department of Chemistry, University of Texas, Austin, Texas 78712 *(Received: May 18, 1988)*

The dark and photocatalytic properties of Ni-doped WS_2 supported on SiO_2 were investigated. Adding Ni increases the dark catalytic hydrogen evolution activity of WS_2. With separate particles of CdS on SiO_2 to photosensitize WS_2/SiO_2, the photocatalytic hydrogen evolution activity of Ni-doped WS_2 maximizes at intermediate Ni loading levels. With fluorescein as a sensitizer, the addition of Ni lowers the activity of WS_2. We interpret the results in terms of a model in which Ni on the *surface* of WS_2 plays an important role in controlling the surface geometric and electronic properties of the substrate and thereby the efficiency of interfacial energy and charge transfer.

Introduction

In a previous paper,[1] we reported catalytic hydrogen evolution properties of silica-supported tungsten disulfide, which we studied using both electrochemical and photocatalytic methods. Although the hydrogen evolution overpotential of WS_2/SiO_2 was larger than that of silica-supported platinum, silica-supported tungsten disulfide was more active and stable than Pt/SiO_2 both in the dark and under visible light illumination in the presence of cadmium sulfide as a sensitizer.

According to the literature, doping of tungsten or molybdenum sulfides with group VIIIB metals (Ni or Co) causes a substantial improvement in their catalytic activity for dehydrogenation and hydrodesulfurization of organic compounds.[2-15] However, different opinions exist concerning the incorporation of nickel (or cobalt) into WS_2 (MoS_2) and its catalytic action. On the basis of both detailed physicochemical and catalytic studies of nickel-

† Permanent address: Institute of Chemical Technology and Engineering, Poznan Technical University, Poznan, Poland.

(1) Sobczynski, A.; Bard, A. J.; Campion, A.; Fox, M. A.; Mallouk, T. E.; Webber, S. E.; White, J. M. *J. Phys. Chem.* **1988**, *92*, 2311.
(2) Voorhoeve, R. J. H.; Stuiver, J. C. M. *J. Catal.* **1971**, *23*, 228.
(3) Voorhoeve, R. J. H.; Stuiver, J. C. M. *J. Catal.* **1971**, *23*, 243.
(4) Farragher, A. L.; Cossee, P. *Proc. Int. Congr. Catal., 5th* **1973**, 130.
(5) Thakur, D. S.; Grange, P.; Delmon, B. *J. Less-Common Met.* **1979**, *64*, 201.
(6) Konings, A. J. A.; van Dooren, A. M.; Koningsberger, D. C.; de Beer, V. J. H.; Farragher, A. L.; Schuit, G. C. A. *J. Catal.* **1978**, *54*, 1.
(7) Konings, A. J. A.; Brentjens, W. L. J.; Koningsberger, D. C.; de Beer, V. J. H. *J. Catal.* **1981**, *67*, 145.
(8) Yermakov, Yu. J.; Startsev, A. N.; Burmistrov, V. A. *Appl. Catal.* **1984**, *11*, 1.
(9) Laihovskii, V. J.; Plyasova, L. M.; Burmistrov, V. A.; Startsev, A. N.; Yermakov, Yu. J. *Appl. Catal.* **1984**, *11*, 15.
(10) Shepelin, A. P.; Zhdan, P. A.; Burmistrov, V. A.; Startsev, A. N.; Yermakov, Yu. J. *Appl. Catal.* **1984**, *11*, 29.

0022-3654/89/2093-0401$01.50/0

and cobalt-doped WS_2 (or MoS_2), several different models of Ni- or Co-doped WS_2 (MoS_2) have been reported.[3,4,15,17-20] The Lipsch and Schuit model[16] assumes the existence of a monolayer of MoS_2 on the Al_2O_3 support, which is formed from a surface aluminum molybdate during the interaction with sulfur. The dopant atoms (Co) are located within the Al_2O_3 layers. In a second model,[3,4] nickel or cobalt is intercalated between the weakly bonded (van der Waals forces) WS_2 or MoS_2 layers. In a third model, Delmon et al.[17-19] assume the existence of two separate phases: WS_2 (MoS_2) and NiS (CoS). In the insertion model,[20] cobalt is located on a lateral face of the MoS_2 crystals. Finally, Yermakov[15] proposed the formation of mixed compounds (nickel and tungsten) on the catalyst surface.

In this paper the catalytic hydrogen evolution properties of nickel-doped tungsten disulfide supported on silica were studied in several different reaction systems, both dark and photochemical. Nickel doping enhances the catalytic properties of WS_2/SiO_2 for dark hydrogen evolution from acidic V^{2+} solution. In photodriven systems, the catalytic action of $Ni-WS_2/SiO_2$ in the presence of various sensitizers depends on the kind of sensitizer. A possible explanation of the observed phenomena is given in terms of interfacial charge and energy transfer which we propose is controlled by Ni on the WS_2 surfaces.

Experimental Section

A. Sample Preparation. Ni-WS_2/SiO_2. In the first step, $WO_3 \cdot nH_2O/SiO_2$ (1.15×10^{-3} mol of WO_3 per 1 g of SiO_2) was prepared in the manner described elsewhere[1,2] and dried at 100 °C. The sample contained 30.5 wt % H_2O as established by conventional gravimetric analysis. Then 1 g of $WO_3 \cdot nH_2O/SiO_2$ was impregnated with an appropriate amount of nickel(II) formate, dried, calcined in air at 400 °C for 3 h, and finally annealed in H_2S at 300 °C for 2 h.

WS_2/SiO_2. WS_2/SiO_2 (without Ni doping) was prepared in a similar way, except that the Ni impregnation step was omitted.

NiS/SiO_2. NiS/SiO_2 was prepared by impregnation of silica (EH-5, Cab-O-Sil) with nickel formate (1.15×10^{-3} mol of Ni^{2+} per 1 g of SiO_2) and was treated similarly to $Ni-WS_2/SiO_2$.

CdS/SiO_2. CdS/SiO_2 was prepared as reported in earlier work.[1,2]

XRD measurements were performed on a Phillips automated powder diffractometer using monochromatized Cu Kα radiation.

B. Experimental Procedures. 1. Dark Catalytic Hydrogen Evolution from V^{2+} Solution. A 0.5 M VCl_3 solution in 30% H_2SO_4 was prepared, and vanadium(III) ions were reduced on Hg/Zn in an argon atmosphere. Twenty milliliters of water was poured into a reaction cell (approximate volume 42 mL). The reaction cell was stoppered with a septum through which two needles penetrated. These allowed for gas flow and sampling for gas chromatography (GC). After the water was deaerated with flowing argon, 10 mL of the V^{2+} solution was injected into it. A catalyst (WS_2/SiO_2, $Ni-WS_2/SiO_2$, or NiS/SiO_2) slurry in water was prepared by sonication of 10 mg of the appropriate powder in 10 mL of water under flowing argon. Then 0.2 mL of the deaerated catalyst slurry was injected into the reaction cell. The cell was kept in the dark, and the reaction mixture was stirred by means of a magnetic stirrer (small, Pyrex-covered bar). Evolving hydrogen was analyzed by GC.[1,2]

2. Hydrogen Photoproduction with a Mixture of CdS/SiO_2 and Ni-WS_2/SiO_2 (WS_2/SiO_2 or NiS/SiO_2) and Methanol as a Sacrificial Electron Donor. Ten milligrams of CdS/SiO_2 and 10 mg of $Ni-WS_2$ (WS_2/SiO_2 or NiS/SiO_2) were mixed with 15 mL of methanol, 12 mL of water, and 3 mL of 1.0 M KOH in a Pyrex reaction cell (42-mL volume). The cell was deaerated as described above. After deaeration (no air contamination by GC), the stirred cell was irradiated with a 1000-W Hg–Xe lamp equipped with a 435-nm cutoff filter and a water jacket. The amount of hydrogen produced was analyzed by GC.

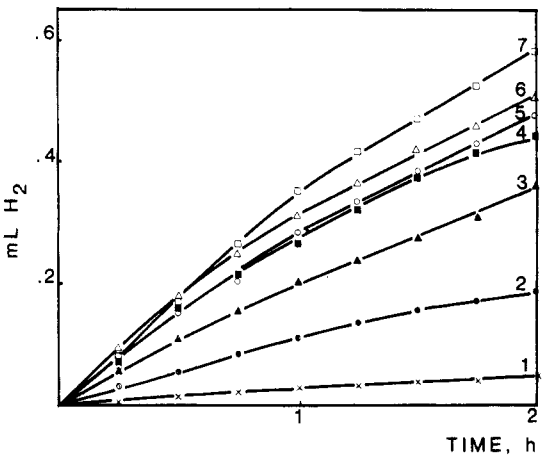

Figure 1. Dark hydrogen evolution from acidic (0.1 M H_2SO_4) V^{2+} solution: (1) NiS/SiO_2, (2) WS_2/SiO_2, (3) 0.07 $Ni-WS_2/SiO_2$, (4) 0.10 $Ni-WS_2/SiO_2$, (5) 0.12 $Ni-WS_2/SiO_2$, (6) 0.15 $Ni-WS_2/SiO_2$, (7) 0.22 $Ni-WS_2/SiO_2$.

3. Hydrogen Photoevolution in the Presence of 1×10^{-4} M Fluorescein and Methanol. A 10-mg sample of the catalyst (Ni/WS_2, WS_2/SiO_2, or NiS/SiO_2) was placed in a reaction cell, and 10 mL of 3.3×10^{-3} fluorescein solution, 15 mL of methanol, and 5 mL of water were added. The cell was deaerated, irradiated with a 1000-W Hg–Xe lamp (420-nm cutoff filter and water jacket), and analyzed for hydrogen evolution by GC.

4. Hydrogen Photoevolution in the Presence of Tris(2,2'-bipyridyl)ruthenium(II) Chloride (Ru(bpy)), Methylviologen Chloride (MV), and Ethylenediaminetetraacetic Acid (EDTA). A 10-mg sample of the catalyst ($NiS-WS_2/SiO_2$, WS_2/SiO_2, or NiS/SiO_2) was placed in a reaction cell, and 0.1117 g of EDTA (disodium salt), 3 mL of 2×10^{-3} M Ru(bpy), 3 mL of 6×10^{-3} M MV, and 24 mL of H_2O were added; the cell was deaerated, illuminated with a 1000-W Hg–Xe lamp (420-nm cutoff filter and water jacket), and analyzed for hydrogen evolution by GC.

Results and Discussion

Pure WS_2/SiO_2, NiS/SiO_2, and five nickel-doped tungsten disulfide samples supported on silica were prepared. The Ni/(Ni + W) ratios were 0.07, 0.10, 0.12, 0.15, and 0.22. The amount of WS_2 was fixed (1.15×10^{-3} mol of WS_2 per 1 g of SiO_2). XRD analysis was performed for WS_2/SiO_2, NiS/SiO_2, and Ni-doped WS_2/SiO_2. All of the Ni-doped WS_2/SiO_2 samples showed only lines characteristic of tungsten disulfide, although their intensities varied from sample to sample. No lines characteristic of NiS were found in any case. As Ni was added, the *c*-axis spacing of WS_2 did not change. All the lines characteristic of WS_2 broadened, suggesting smaller crystallites when Ni was added. This suggests a solid solution at the surface of NiS in WS_2 rather than two separate phases. Because the *c*-axis spacing was constant, a bulk solid solution is unlikely. However, it is impossible to determine, on the basis of powder XRD analysis alone, which sites in WS_2 are occupied by nickel ions.

The results of a dark catalytic hydrogen evolution from acidic V^{2+} solution (0.1 M H_2SO_4) are shown in Figure 1 and in Figure 2 (curve 2). Nickel doping clearly enhances the catalytic properties of WS_2 for dark hydrogen evolution. By comparison, the hydrogen evolution properties of NiS/SiO_2 (Figure 1) are very poor. The rate of H_2 evolution on WS_2/SiO_2 was 120 μL h^{-1} whereas on 0.22 $Ni-WS_2/SiO_2$ (the most active sample) the rate was 350 μL h^{-1}. Because of deteriorating photochemical properties (see below), we did not pursue higher Ni loadings. Thus, adding nickel modifies the properties of WS_2. Based on the XRD data, the

(11) Thakur, D. S.; Delmon, B. *J. Catal.* **1985**, *91*, 308.
(12) Thakur, D. S.; Grange, P.; Delmon, B. *J. Catal.* **1985**, *91*, 318.
(13) Delamay, F. *Appl. Catal.* **1985**, *16*, 135.
(14) Yermakov, Yu. J.; Startsev, A. N.; Burmistrov, V. A.; Shumilo, O. N.; Bulgakov, N. N. *Appl. Catal.* **1985**, *18*, 33.
(15) Yermakov, Yu. J. *Usp. Khim.* **1986**, *55*, 499.
(16) Lipsch, J. M.; Schuit, G. C. A. *J. Catal.* **1969**, *15*, 179.
(17) Delmon, B. *Bull. Soc. Chim. Belg.* **1979**, *88*, 979.
(18) Grange, P.; Delmon, B. *J. Less-Common Met.* **1974**, *36*, 353.
(19) Hagenbach, G.; Courly, P.; Delmon, B. *J. Catal.* **1973**, *31*, 264.
(20) Radnasamy, P.; Sivasankev, S. *Catal. Rev—Sci. Eng.* **1980**, *22*, 401.
(21) Sobczynski, A.; Bard, A. J.; Campion, A.; Fox, M. A.; Mallouk, T. E.; Webber, S. E.; White, J. M. *J. Phys. Chem.* **1987**, *91*, 3316.

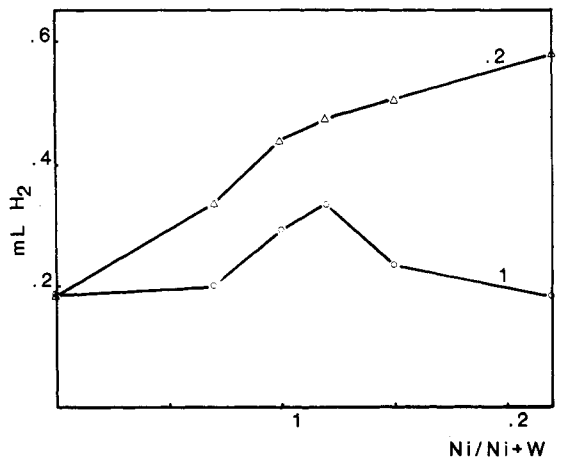

Figure 2. Dependence of hydrogen evolution on Ni/(Ni + W) ratio in Ni-WS_2/SiO_2: (1) from water–methanol–KOH under irradiation in the presence of CdS/SiO_2 as a sensitizer; (2) from V^{2+} acidic solution (in dark).

modification may be the result of adding some NiS to the WS_2 lattice or the result of formation of a solid solution (or a new compound) on the surface of silica-supported tungsten disulfide.

The results of hydrogen photoproduction with a mixture of CdS/SiO_2 and Ni-WS_2/SiO_2 from water–methanol–KOH solution are shown in Figure 2 (curve 1). The activity attains a maximum with Ni/(Ni + W) = 0.12. All nickel-doped samples are more active than undoped WS_2/SiO_2. The NiS/SiO_2 (not shown) shows an activity about 2 times lower than undoped WS_2/SiO_2. The difference in the hydrogen evolution activity of Ni-WS_2/SiO_2 in the dark experiment with V^{2+} acidic solution and under visible light irradiation using separate particles of CdS/SiO_2 as a sensitizer can be understood if we assume that, in the latter case, the interaction of the two separately supported components plays a role in the overall activity. It was shown in our previous paper[21] that agglomeration of CdS/SiO_2 and Pt/SiO_2 played an essential role in hydrogen evolution from water–methanol–KOH.

Our results here show that, although the catalytic hydrogen evolution properties of Ni-WS_2/SiO_2 increase with added nickel, the interaction of CdS/SiO_2 with Ni-WS_2/SiO_2 becomes poorer at higher nickel loading. The reasons are unclear, but one possibility is that added Ni has two effects which oppose each other: (1) it quenches the excited state of CdS, and (2) it catalyzes H_2 evolution. Another possibility is that Ni decreases the interaction between particles containing CdS and those containing Ni-WS_2.

The most surprising results were obtained with fluorescein as a sensitizer and methanol as a sacrificial electron donor. Only undoped WS_2/SiO_2 evolved hydrogen, and the average (4 h of illumination) rate was 25 $\mu L\ h^{-1}$. Neither the nickel-doped samples nor the NiS/SiO_2 was active. A little hydrogen was evolved during the first 30 min of illumination. However, a similar amount was observed at the beginning of illumination of the catalysts in water–methanol (with and without KOH) with no sensitizers present. This small amount of hydrogen is attributed to a photochemical reaction between the WS_2 surface and the methanol–water solution. The absence of activity for all the nickel-doped WS_2/SiO_2 samples suggests that the surface sites and the accompanying local electronic structure responsible for the interaction between WS_2 and fluorescein are significantly altered,

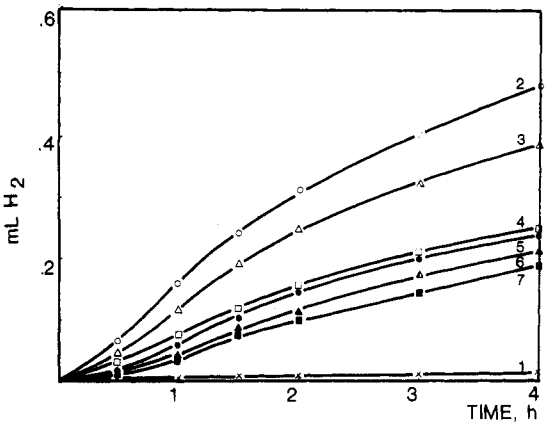

Figure 3. Visible light hydrogen evolution in the presence of 2×10^{-4} M $Ru(bpy)_3^{2+}$, 6×10^{-4} MV^{2+}, and 1×10^{-2} Na_2EDTA: (1) NiS/SiO_2, (2) WS_2/SiO_2, (3) 0.07 Ni-WS_2/SiO_2, (4) 0.10 Ni-WS_2/SiO_2, (5) 0.12 Ni-WS_2/SiO_2, (6) 0.15 Ni-WS_2/SiO_2, (7) 0.22 Ni-WS_2/SiO_2.

perhaps even occupied, by nickel atoms on the surface.

The results of H_2 evolution from a 0.01 M EDTA (disodium salt) solution in the presence of tris(2,2′-bipyridyl)ruthenium(II) chloride as a sensitizer and methylviologen chloride as an electron relay are shown in Figure 3. Clearly, despite changes in the activity at the beginning of illumination (which are due to the varying extent of H_2 adsorption by the catalyst; see the discussion in our previous paper[1]), the activities of the catalysts (except NiS/SiO_2) are nearly the same over the time period 2–4 h. Moreover, the activities of the undoped WS_2/SiO_2 and all nickel-doped samples were nearly the same (14–18 $\mu L\ h^{-1}$) over the time period 4–20 h (not shown in Figure 3). Keeping in mind that the hydrogen evolution activity of Ni-WS_2/SiO_2 is much better than that of undoped WS_2/SiO_2 and that it increases with nickel content, it seems likely that, in this case, hydrogen evolution does not control the rate and that Ni does not alter charge transfer from the relay to WS_2.

Summing up these results, we conclude that nickel doping improves the catalytic hydrogen evolution properties of silica-supported tungsten disulfide but that the enhancement of photosensitization efficiency is very dependent on the sensitizer. For CdS/SiO_2 as a sensitizer, small amounts of Ni doping of WS_2/SiO_2 are beneficial. The features are similar to our earlier work on WS_2/SiO_2–CdS/SiO_2.[1] On the other hand, nickel doping does not work well when organic molecules are used either to absorb light or as relays. Although we did not perform systematic structural and physicochemical studies of Ni-WS_2/SiO_2, the very different behavior of the various systems allows us to draw some conclusions regarding the nickel distribution in the catalysts. Our results suggest the importance of Ni on the surface of WS_2, as in the model proposed by Yermakov.[15] This does not exclude the buildup of tiny nickel deposits between WS_2 layers (intercalation model[3,4]), but these cannot change the c-axis spacing of WS_2. While we did not investigate other cases, we expect that other metals, such as Co and Mo, may function similarly.

Acknowledgment. This work was supported by the Gas Research Institute.

Registry No. H_2, 1333-74-0; Ni, 7440-02-0; WS_2, 12138-09-9; SiO_2, 7631-86-9; H_2O, 7732-18-5; NiS, 11113-75-0; CH_3OH, 67-56-1; MV, 1910-42-5; Na_2EDTA, 139-33-3; V^{2+}, 15121-26-3; $Ru(bpy)_3^{2+}$, 15158-62-0; fluorescein, 2321-07-5.